Supporting information

Three N-stablization rhodamine-based fluorescent probe for Al^{3+} via Al^{3+}-promoted hydrolysis of Schiff base

Peigang Ding[a], Jinhui Wang[a], Junye Cheng[a], Yufen Zhao[a-c], Yong Ye [a,c]*

[a] *Phosphorus Chemical Engineering Research Center of Henan Province, the College of Chemistry and Molecular Engineering, Zhengzhou University, Zhengzhou 450052, China.*

[b] *Key Laboratory for Chemical biology of Fujian Province, Xiamen University, Xiamen 361005, China.*

[c] *Key Laboratory of Bioorganic Phosphorus Chemistry & Chemical Biology(Ministry of Education), Department of Chemistry, Tsinghua University, Beijing 100084, China.*

**Corresponding author. E-mail address: yeyong03@tsinghua.org.cn (Yong Ye).*

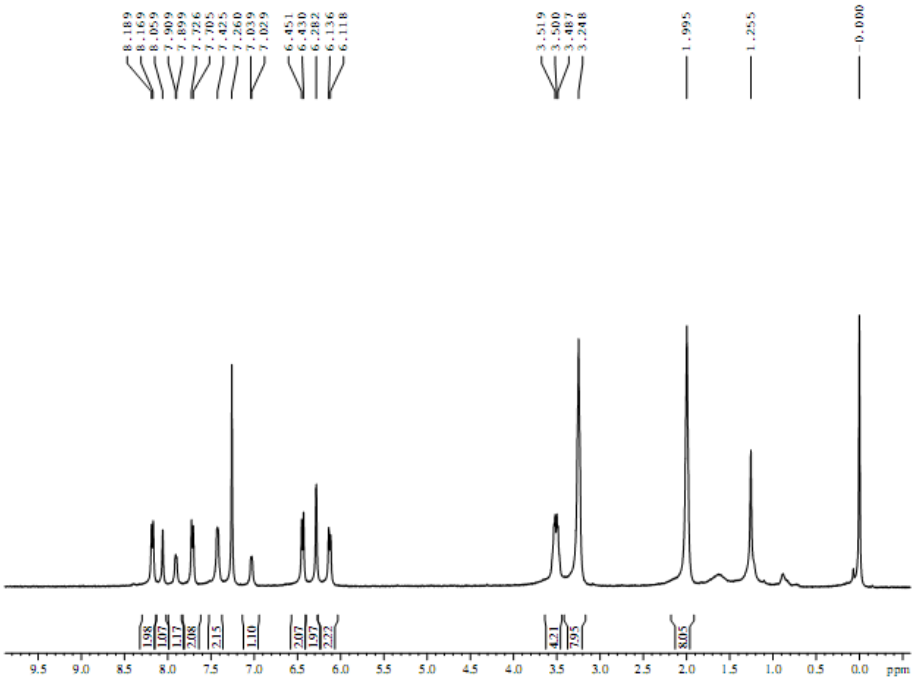

Fig. S1. ^{1}H NMR spectrum of $\mathbf{L_1}$ in $CDCl_3$.

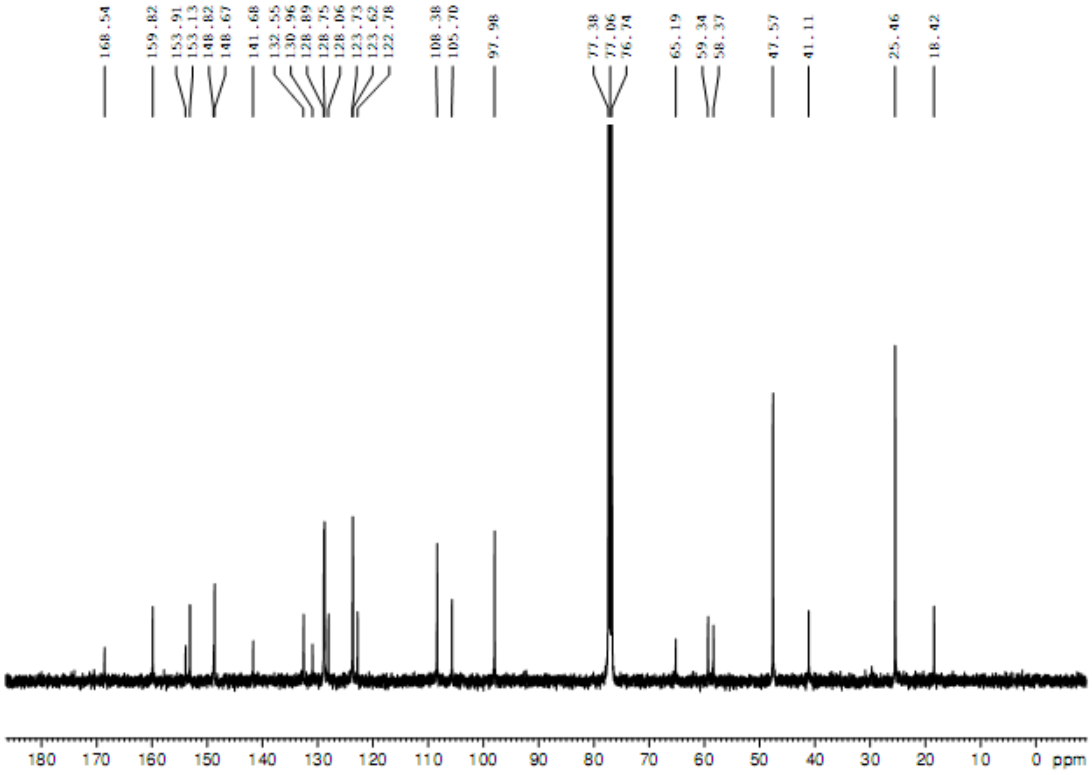

Fig. S2. ^{13}C NMR spectrum of $\mathbf{L_1}$ in $CDCl_3$.

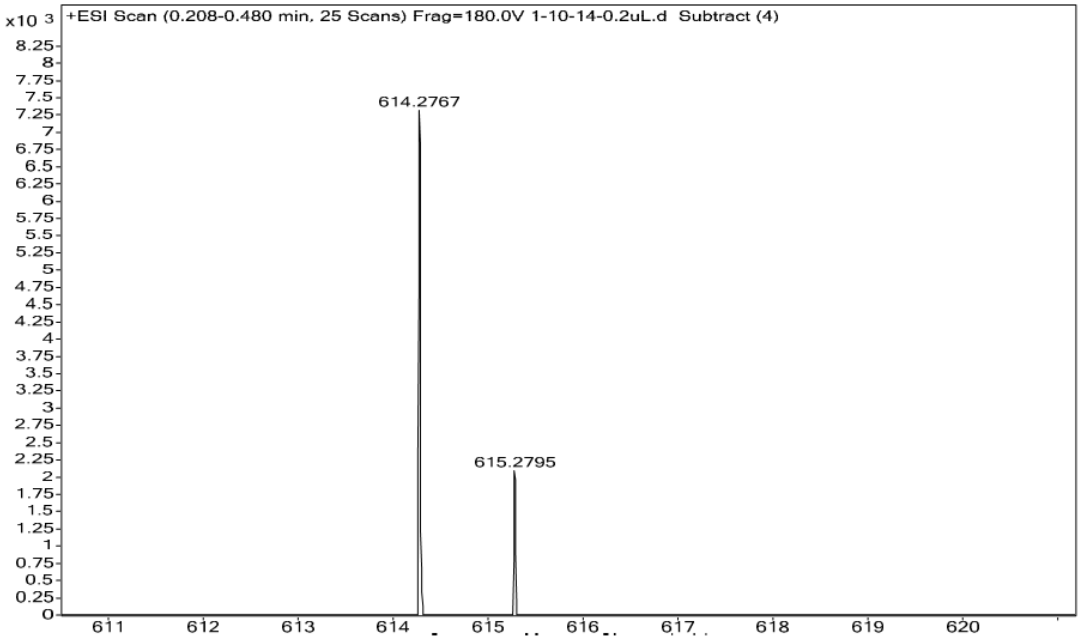

Fig. S3. HRMS of $\mathbf{L_1}$.

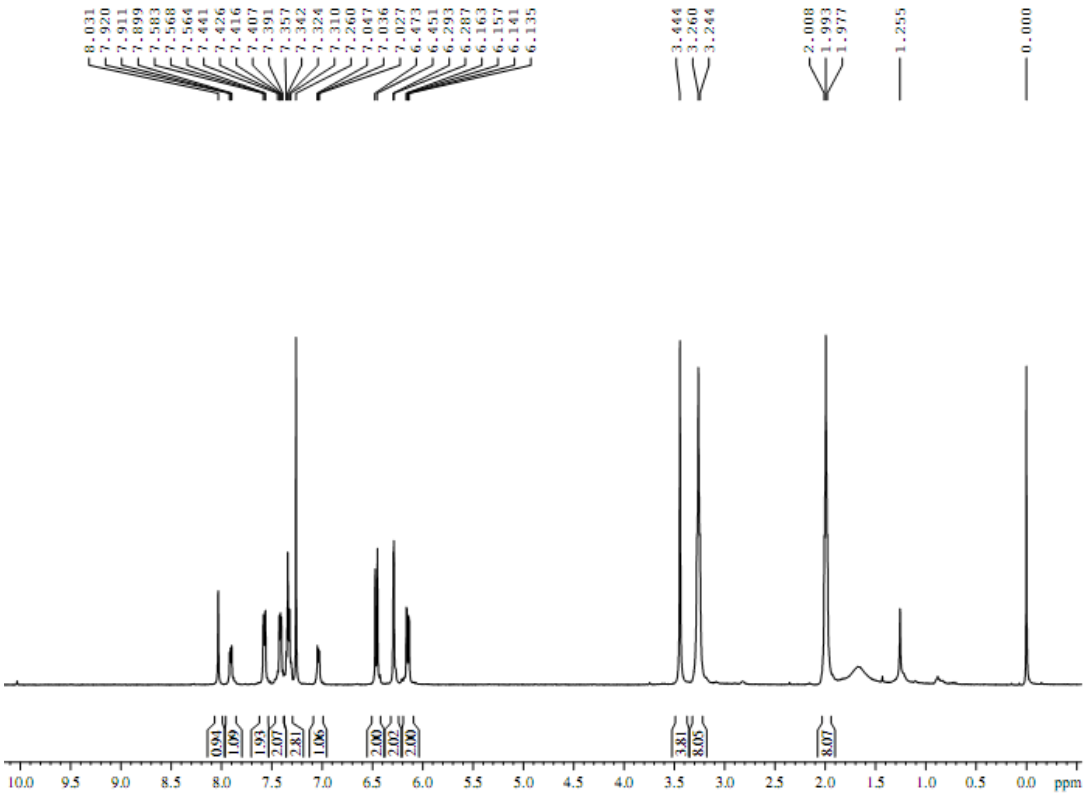

Fig. S4. ^{1}H NMR spectrum of $\mathbf{L_2}$ in $CDCl_3$.

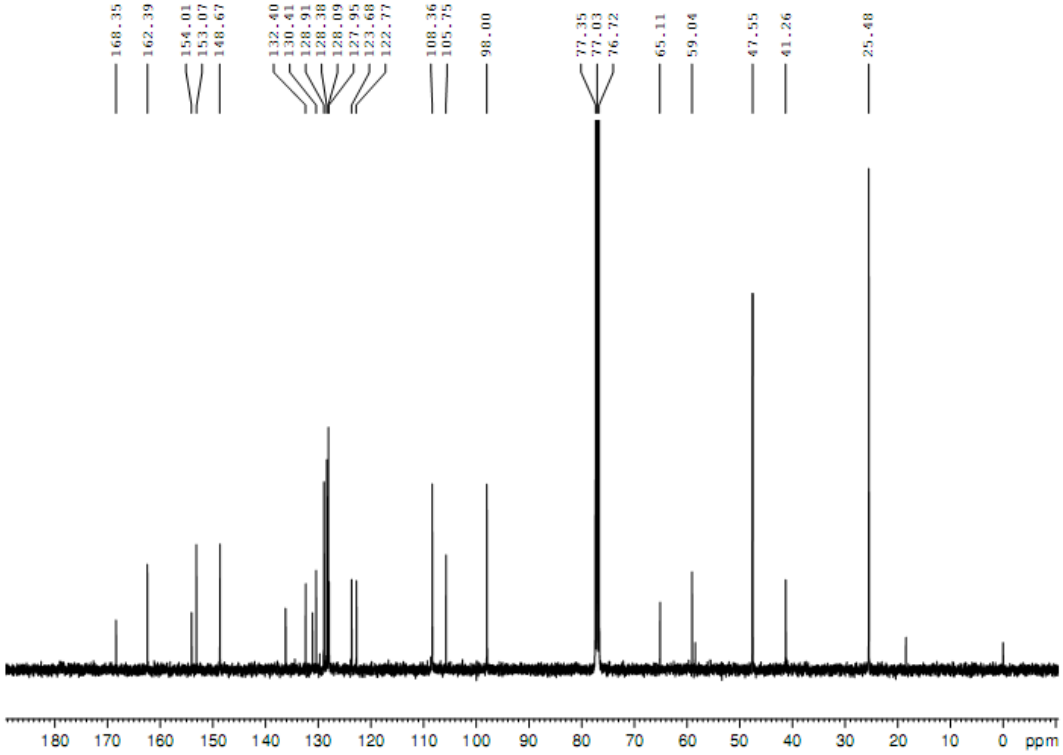

Fig. S5. ^{13}C NMR spectrum of $\mathbf{L_2}$ in $CDCl_3$.

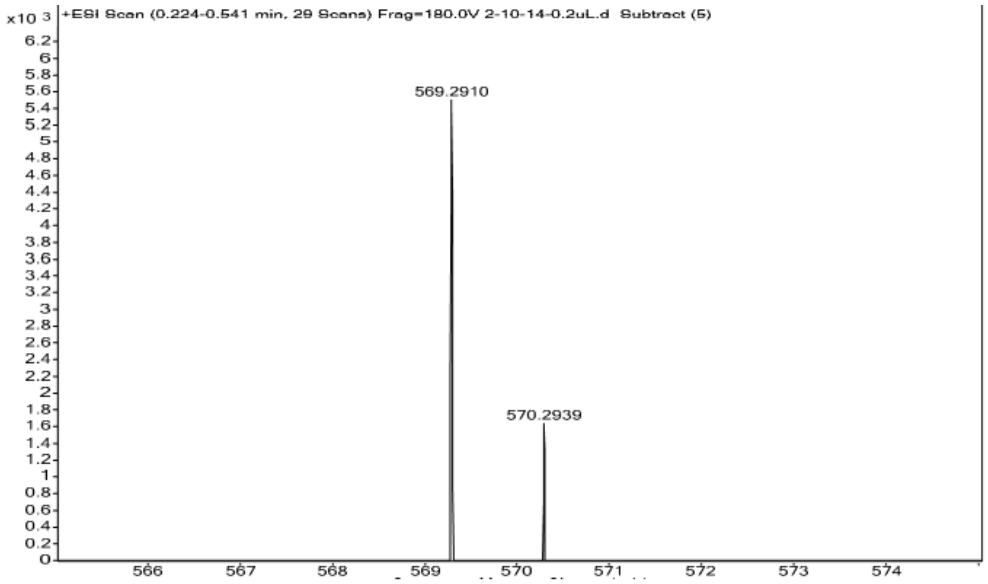

Fig. S6. HR-MS of $\mathbf{L_2}$.

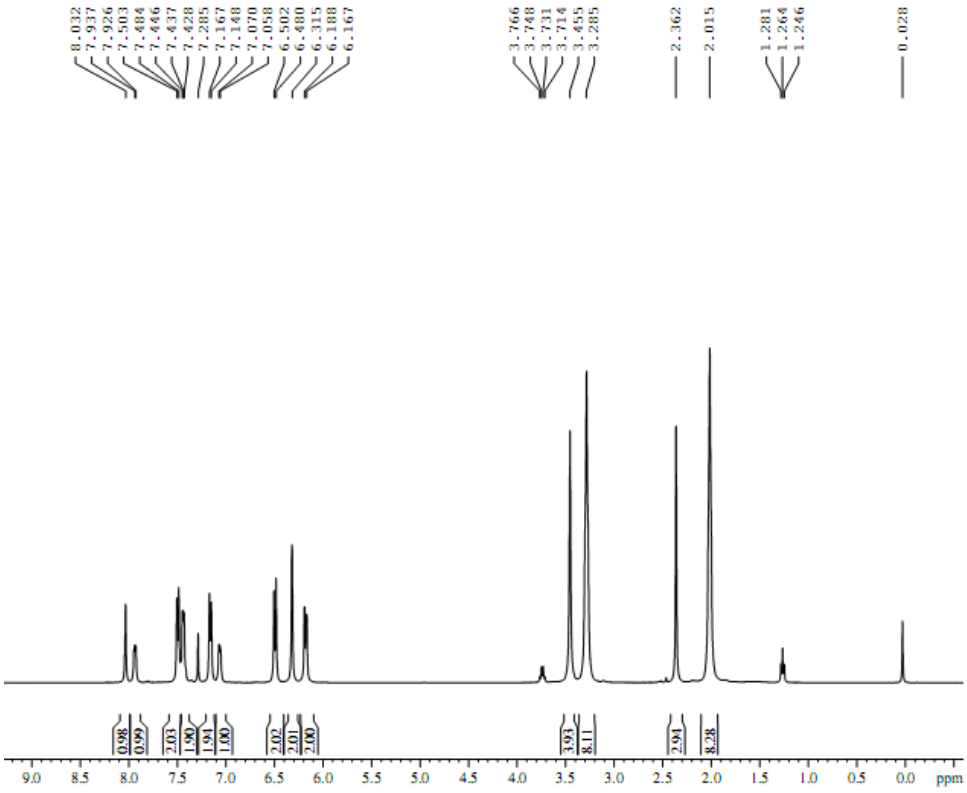

Fig. S7. ^{1}H NMR spectrum of $\mathbf{L_3}$ in $CDCl_3$

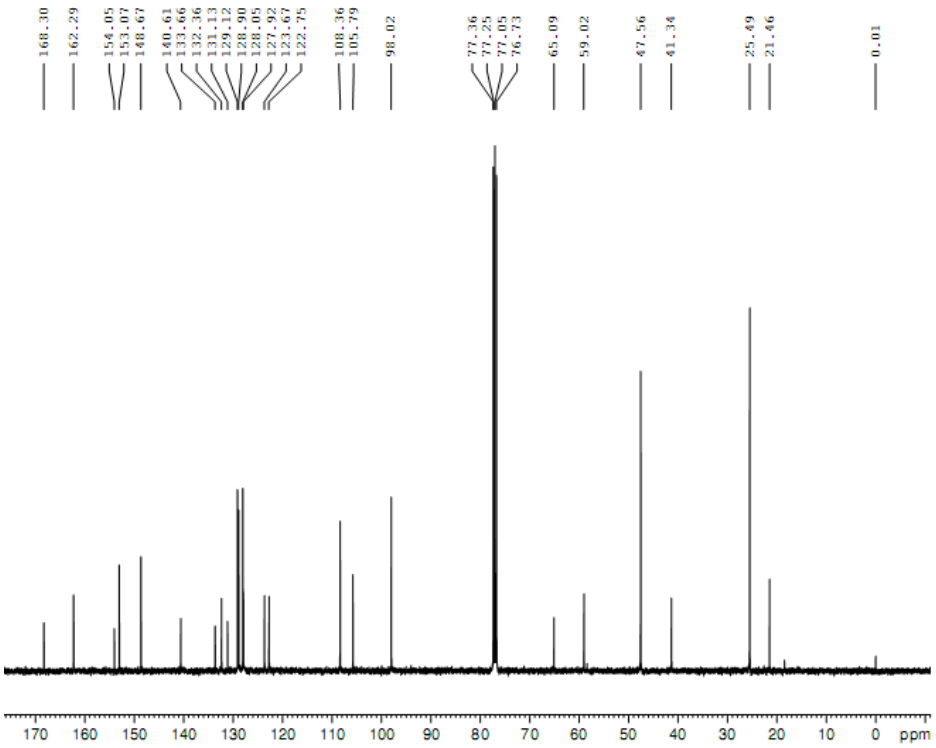

Fig. S8. ^{13}C NMR spectrum of $\mathbf{L_3}$ in $CDCl_3$.

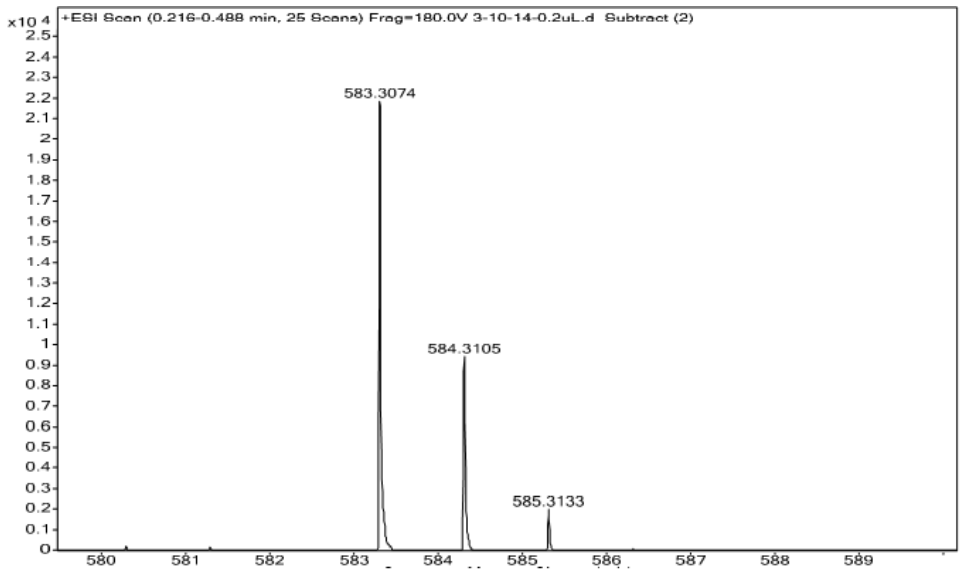

Fig. S9. HR-MS of $\mathbf{L_3}$.

compound	Φfs	compound	Φfs
$\mathbf{L_1}$	0.003	$\mathbf{L_1}$ + Al^{3+}	0.59
$\mathbf{L_2}$	0.004	$\mathbf{L_2}$ + Al^{3+}	0.47
$\mathbf{L_3}$	0.005	$\mathbf{L_3}$ + Al^{3+}	0.29

Fig. S10. The fluorescence quantum yield of $\mathbf{L_1}$, $\mathbf{L_2}$, $\mathbf{L_3}$, $\mathbf{L_1}$ + Al^{3+}, $\mathbf{L_2}$ + Al^{3+} and $\mathbf{L_3}$ + Al^{3+}. The fluorescence quantum yield was measured at room temperature with excitation at 495 nm (Xe lamp in the HITACHI F-4500 spectrometer) with rhodamine B (Φ_{fs} = 0.89) selected as the reference.

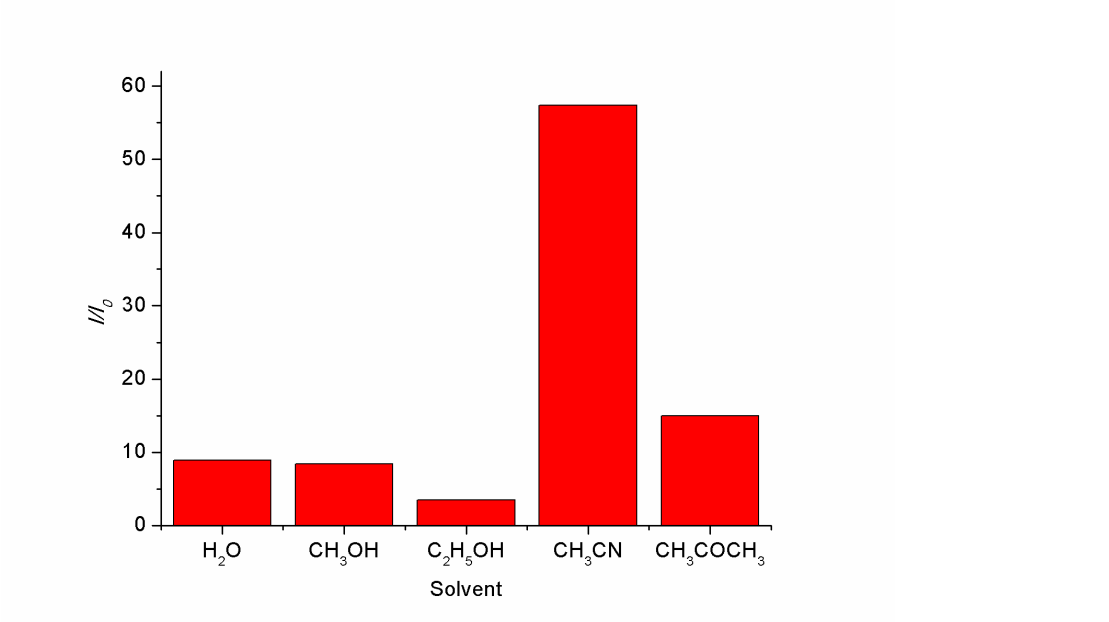

Fig. S11. I: Fluorescence intensity (at 582 nm) of $\mathbf{L_1}$ (10 μM) in different solvent with the presence of Al^{3+} (100 μM) (λex = 520 nm); I_0: Fluorescence intensity (at 582 nm) of free $\mathbf{L_1}$ (10 μM) in corresponding different solvent (λex = 520 nm).

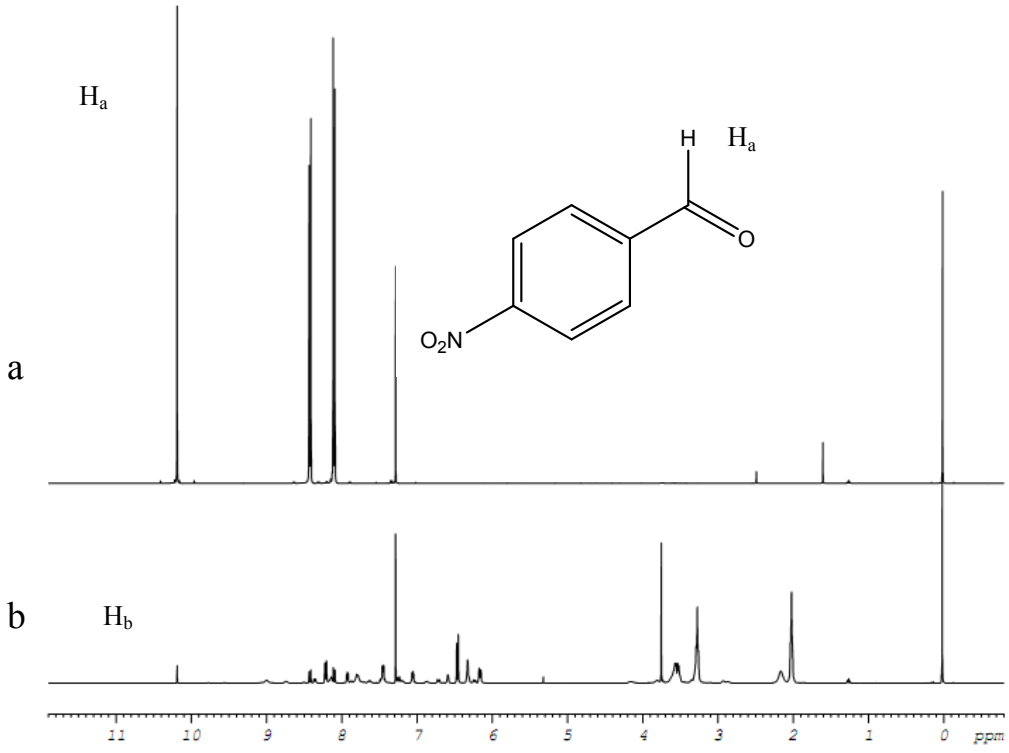

Fig. S12. ^{1}H NMR spectra of p-nitrobenzaldehyde (a) and $\mathbf{L_1}$ + Al^{3+} (b) in $CDCl_3$.

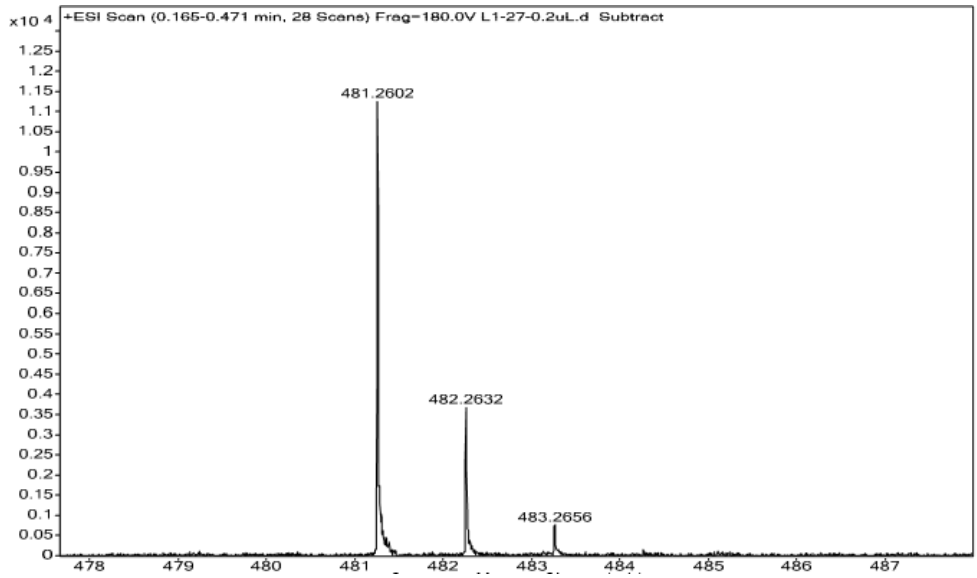

Fig. S13. HR-MS of $\mathbf{L_1}$ in the presence of Al^{3+} in CH_3CN/H_2O (95:5, v/v) solution.

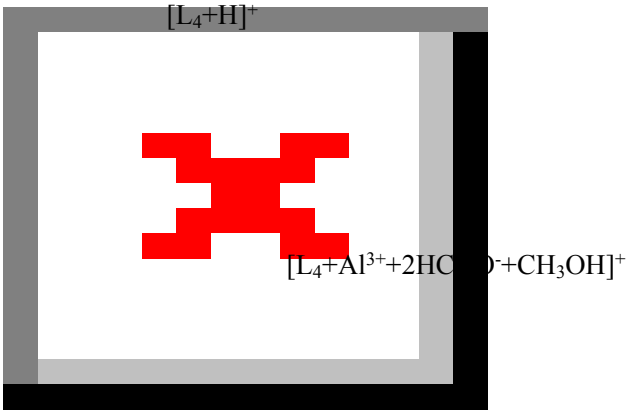

Fig. S14. ESI-MS of $\mathbf{L_1}$ in the presence of Al^{3+}.

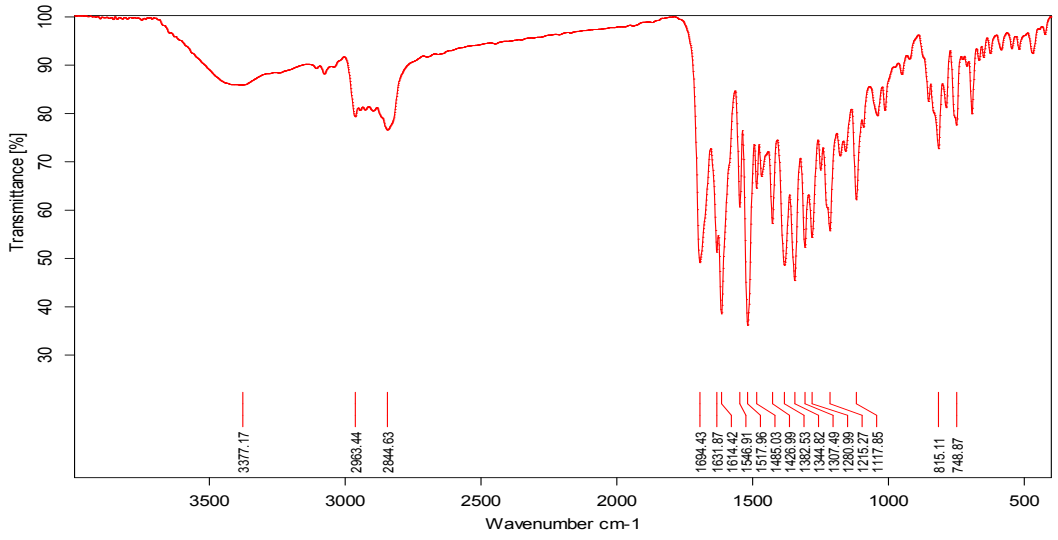

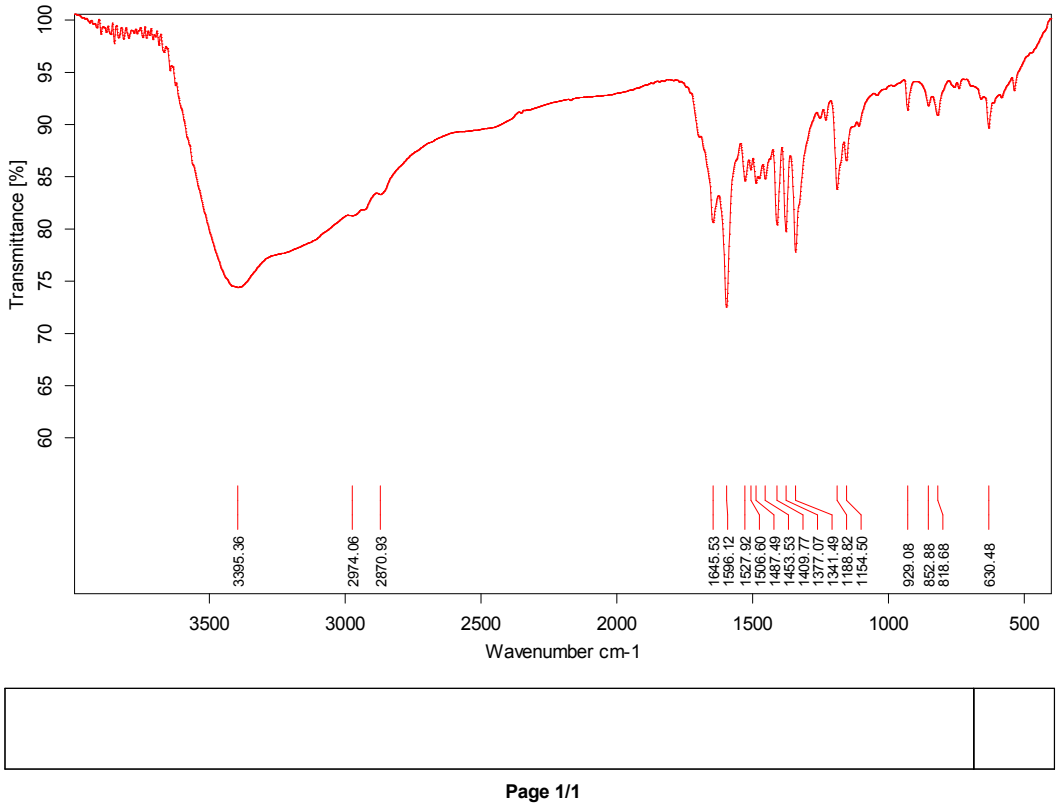

Fig.S15. IR spectra of free (upper) L_1 and (down) L_1+ Al^{3+} in CH_2Cl_2.

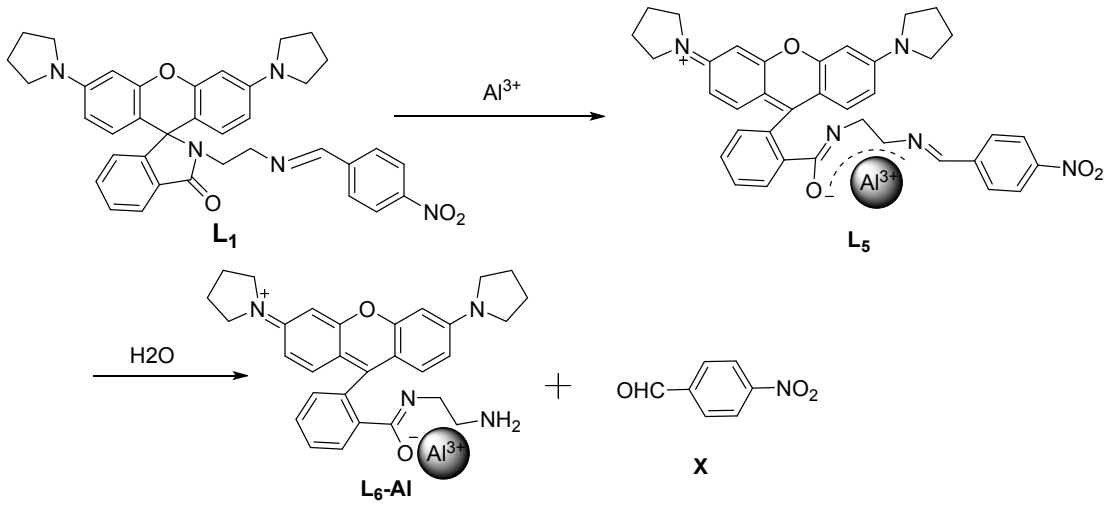

Supporting information

Optimized structures and Cartesian coordinates of **L5**, **H_2O**, **L6** and **p-nitrobenzaldehyde**

L5

Energy= -3168.534535 a.u.

C	4.98717400	-1.74620600	0.09602300
C	4.21902600	-0.93260400	0.88186700

C	3.40991000	0.10807900	0.33126600
C	3.43738600	0.23127700	-1.09160100
C	4.20483700	-0.57490600	-1.90493500
C	5.01205700	-1.59100500	-1.33324900
C	2.58527200	0.97438300	1.08395500
C	1.87707200	2.01849300	-1.01751100
C	1.81941000	1.95023700	0.40842200
C	0.99456700	2.92743800	1.04499400
H	0.94661500	2.95097100	2.12713100
C	0.27298000	3.84260300	0.33050600
C	0.31857000	3.86765900	-1.10661900
C	1.15713700	2.92940800	-1.76043600
H	5.59248700	-2.51335100	0.56197600
H	4.15844600	-0.42122100	-2.97504300
H	-0.32533800	4.57282700	0.86030200
H	1.24757100	2.90233800	-2.83841400
O	2.67292900	1.16573100	-1.71986700
C	6.56914200	-3.52743900	-1.59299700
C	5.90956600	-2.23696400	-3.56156500
C	6.97858900	-4.27972500	-2.86562100
H	5.97038700	-4.14280100	-0.91540100
H	7.44368100	-3.15862200	-1.04114800
C	7.07346800	-3.16862900	-3.92216700
H	4.97723200	-2.53966700	-4.05706500
H	6.10815500	-1.19178000	-3.81809900
H	7.91431000	-4.82809700	-2.73120700
H	6.99578800	-3.54064500	-4.94676200
N	5.77576600	-2.39076100	-2.10119100
H	6.19902500	-4.99902100	-3.14002700
H	8.02415600	-2.63253000	-3.82609300
C	2.57633600	0.89976200	2.57396200
C	1.42175200	0.59359400	3.32984400
C	3.75629700	1.23492900	3.25695600
C	1.47089400	0.65211400	4.73075000
C	3.79925500	1.26711400	4.65005200
H	4.64039600	1.49653200	2.68427000
C	2.65336900	0.97528100	5.39075900
H	0.57125400	0.42972400	5.29457900
H	4.72500200	1.53131500	5.15186900
H	2.67706700	1.00433500	6.47553900
C	-1.35723800	5.71627600	-1.19892900
C	-0.34679600	4.90124100	-3.27012600
C	-2.14355700	6.25208400	-2.40200600
H	-0.81324700	6.51747000	-0.68156600

H	-1.99663800	5.20962500	-0.47077000
C	-1.12349900	6.19484300	-3.54899300
H	-0.82046400	4.03107500	-3.74395400
H	0.69244300	4.95079600	-3.60964400
H	-2.99269300	5.59317600	-2.61484000
H	-2.53140800	7.25745500	-2.21989000
H	-1.58761300	6.18605000	-4.53833600
H	-0.44608700	7.05455300	-3.49912500
N	-0.40316400	4.76550100	-1.80288100
C	0.11570700	0.21073700	2.73223600
O	-0.97512600	0.75526900	3.15754700
N	-0.12676500	-0.69600000	1.80172100
C	0.58113900	-1.79284300	1.18559800
C	-0.46601900	-2.92182200	1.10618100
H	1.45243300	-2.12369700	1.75945200
H	0.91346300	-1.51877000	0.17816300
H	-0.17794600	-3.68537700	0.37805300
H	-0.55874100	-3.39719000	2.08935300
N	-1.80328700	-2.35662300	0.78820000
C	-2.45169400	-2.91668200	-0.17115100
H	-1.95281600	-3.70320100	-0.74423600
C	-3.82637400	-2.62657500	-0.60087700
C	-4.82639100	-2.18519200	0.28222400
C	-4.14900100	-2.87713200	-1.94735100
C	-6.12001400	-1.96761500	-0.17685900
H	-4.60400400	-2.04369900	1.33295500
C	-5.43404400	-2.64409200	-2.42237800
H	-3.38723700	-3.24469400	-2.62797000
C	-6.39918400	-2.19080200	-1.52462800
H	-6.90402100	-1.63614800	0.49165200
H	-5.69258400	-2.81682600	-3.45896900
N	-7.76568300	-1.95527400	-2.01360800
O	-7.99801400	-2.16975100	-3.20399200
O	-8.60647300	-1.55454900	-1.20795000
Al	-2.00621500	-0.56865000	1.97425800
Cl	-3.16568100	-1.46896400	3.58680400
Cl	-3.09493100	0.78512300	0.68420200
H	4.22492300	-1.07860600	1.95564700

H_2O

Energy= -76.4161195 a.u.

O	0.00000000	0.00000000	0.12071700
H	0.00000000	0.75887200	-0.48286700
H	0.00000000	-0.75887200	-0.48286700

L6

Energy= -2694.8933548 a.u.

C	4.20196100	-0.60470900	0.64114300
C	2.94883400	-0.81688900	1.14513900
C	1.88435200	0.11457200	0.94525900
C	2.20582600	1.27011100	0.16964600
C	3.46123000	1.50716000	-0.34820200
C	4.50553000	0.57443600	-0.12377300
C	0.56605300	-0.05076500	1.42578200
C	-0.01990700	2.07401300	0.35431700
C	-0.39708600	0.94229200	1.14043600
C	-1.74561400	0.93327600	1.61132900
H	-2.07599600	0.11914700	2.24553400
C	-2.62933100	1.92788000	1.29670300
C	-2.23373800	3.04302900	0.47937400
C	-0.89185600	3.08902800	0.02364000
H	4.97797500	-1.33559600	0.82979900
H	3.61639800	2.40314300	-0.93467600
H	-3.63723800	1.88236800	1.68927700
H	-0.52727800	3.90315500	-0.58884600
O	1.25387300	2.20177700	-0.10956600
C	6.85480200	-0.18513100	-0.50490400
C	6.14289000	1.99930500	-1.33957600
C	7.90575200	0.36361400	-1.47824900
H	6.51970300	-1.19142000	-0.77207400
H	7.23161600	-0.21004000	0.52603900
C	7.66894300	1.88083400	-1.44020100
H	5.66982400	2.01757300	-2.33067100
H	5.82281200	2.89147700	-0.79247900
H	8.91940700	0.07782100	-1.18642200
H	8.06091000	2.40020300	-2.31819000
N	5.74255600	0.77965900	-0.61385500
H	7.71934400	-0.02475800	-2.48564300
H	8.13660600	2.31683300	-0.55041700
C	0.21884400	-1.22321300	2.28074700
C	-0.73747000	-2.19860900	1.91668300
C	0.81671600	-1.30880600	3.54816400
C	-1.08207700	-3.20834200	2.82860900
C	0.48195900	-2.32971100	4.43655800
H	1.53357500	-0.54978800	3.84502600
C	-0.47100600	-3.28332600	4.07697000
H	-1.82873000	-3.93927000	2.53813500
H	0.95886300	-2.37020100	5.41102600

H	-0.74123100	-4.07797200	4.76523400
C	-4.54059700	3.99862700	0.53721900
C	-2.75180100	5.23319400	-0.58157300
C	-5.14196400	5.13520600	-0.29949400
H	-4.65657700	4.18364200	1.61321800
H	-4.98391300	3.02601700	0.30594000
C	-3.98297500	6.13494200	-0.42794500
H	-2.56144000	4.97933700	-1.63304500
H	-1.84356900	5.68403300	-0.16971000
H	-5.43005500	4.75830600	-1.28714800
H	-6.02986200	5.56277300	0.17294300
H	-4.09525600	6.81872500	-1.27303200
H	-3.89454500	6.73444900	0.48486500
N	-3.11022600	4.01737700	0.17200000
C	-1.43095600	-2.23629100	0.60341500
O	-2.70276700	-2.48565000	0.55761600
N	-0.92625900	-2.09713500	-0.60727100
C	0.36951200	-2.12892900	-1.24548700
C	0.15273000	-2.95748500	-2.53360800
H	1.14900100	-2.58951700	-0.63042800
H	0.69221900	-1.11241300	-1.50013400
H	0.92953200	-2.75049300	-3.27392800
H	0.17236200	-4.02378400	-2.29517000
N	-1.21083100	-2.66569500	-3.08608200
Al	-2.54522000	-2.61487300	-1.46389000
Cl	-3.24015900	-4.67638500	-1.66618400
Cl	-3.97586500	-1.13900300	-2.16868800
H	-1.20713200	-1.76018500	-3.56188100
H	-1.44541200	-3.35486300	-3.80144600
H	2.75549500	-1.71811200	1.71501600

p-nitrobenzaldehyde

Energy= -550.0806347 a.u.

C	0.91664800	1.37677300	-0.00000200
C	-0.47203700	1.28097400	0.00000100
C	-1.04505000	0.01032300	-0.00000600
C	-0.28419700	-1.16136900	-0.00001800
C	1.09973700	-1.04927200	-0.00001900
C	1.70452900	0.21767400	-0.00000900
H	1.38984600	2.35465800	0.00000500
H	-1.10198900	2.16110900	0.00000800
H	-0.77563900	-2.12587100	-0.00002600
H	1.72708600	-1.93428800	-0.00002600
N	-2.51246200	-0.10125400	-0.00001100

O	-3.00594800	-1.22968200	0.00006300
O	-3.17172400	0.93907100	-0.00003400
C	3.18435700	0.33921500	0.00000300
O	3.94703800	-0.61079400	-0.00001600
H	3.56908500	1.37849500	0.00030700

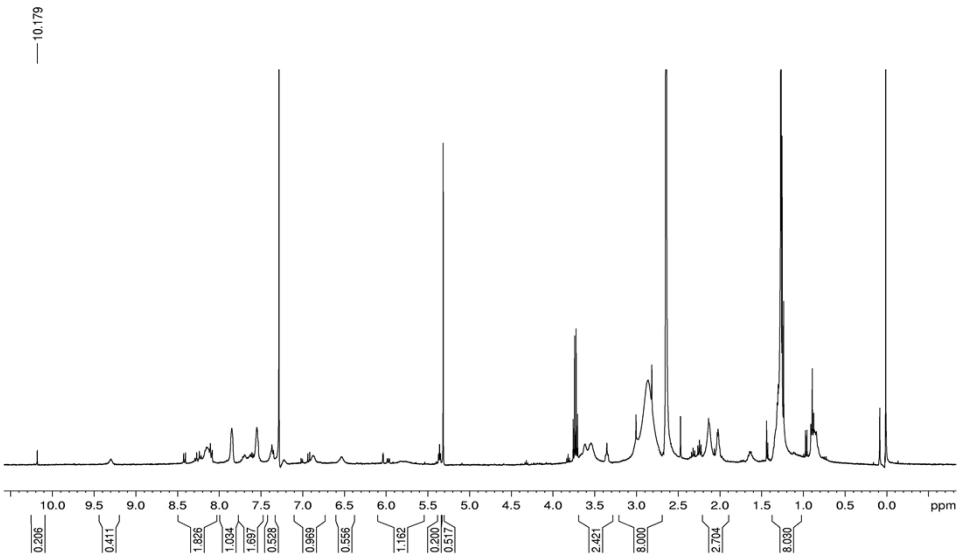

Fig. S16. ^{1}H NMR spectra of $\mathbf{L_1}$ + Fe^{3+} in $CDCl_3$.

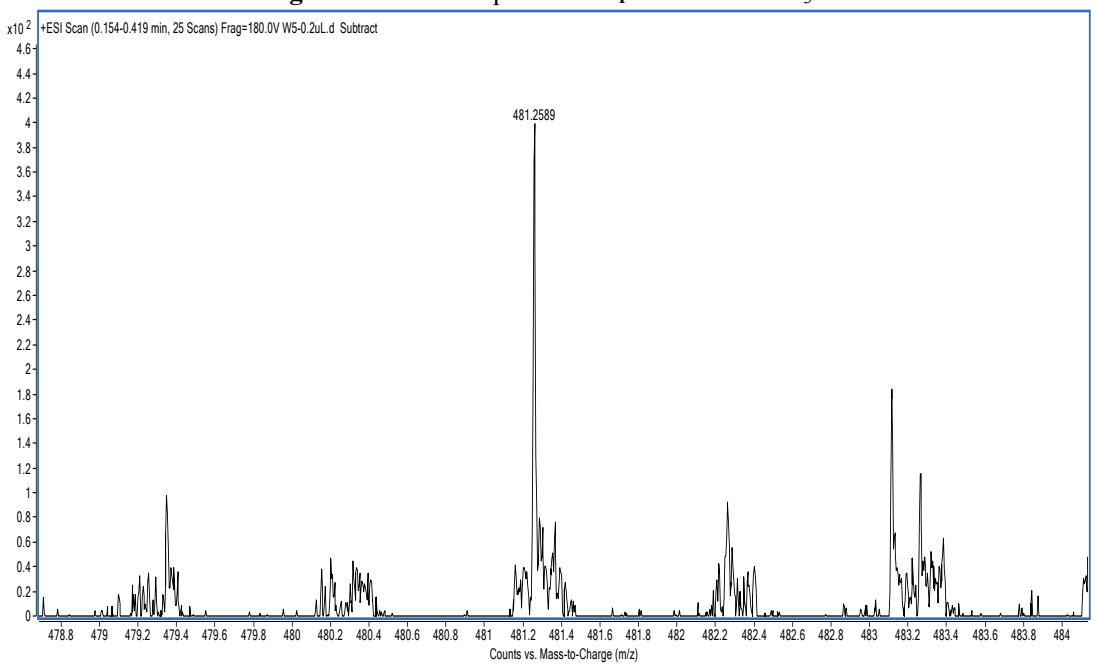

Fig. S17. HR-MS of $\mathbf{L_1}$ in the presence of Fe^{3+} in CH_3CN/H_2O (95:5, v/v) solution.

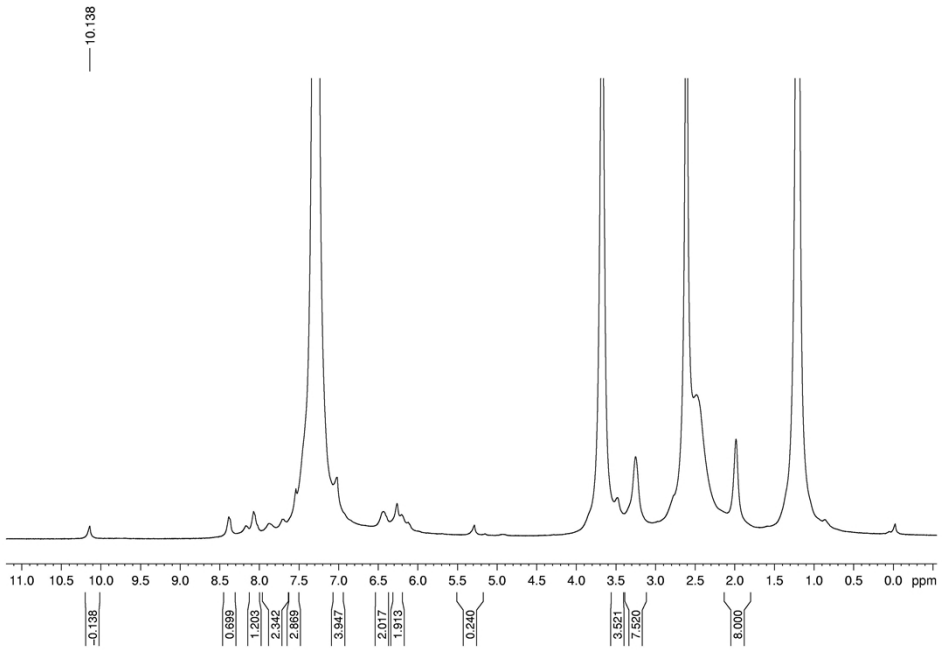

Fig. S18. ^{1}H NMR spectra of $\mathbf{L_1}$+Cr^{3+} in $CDCl_3$.

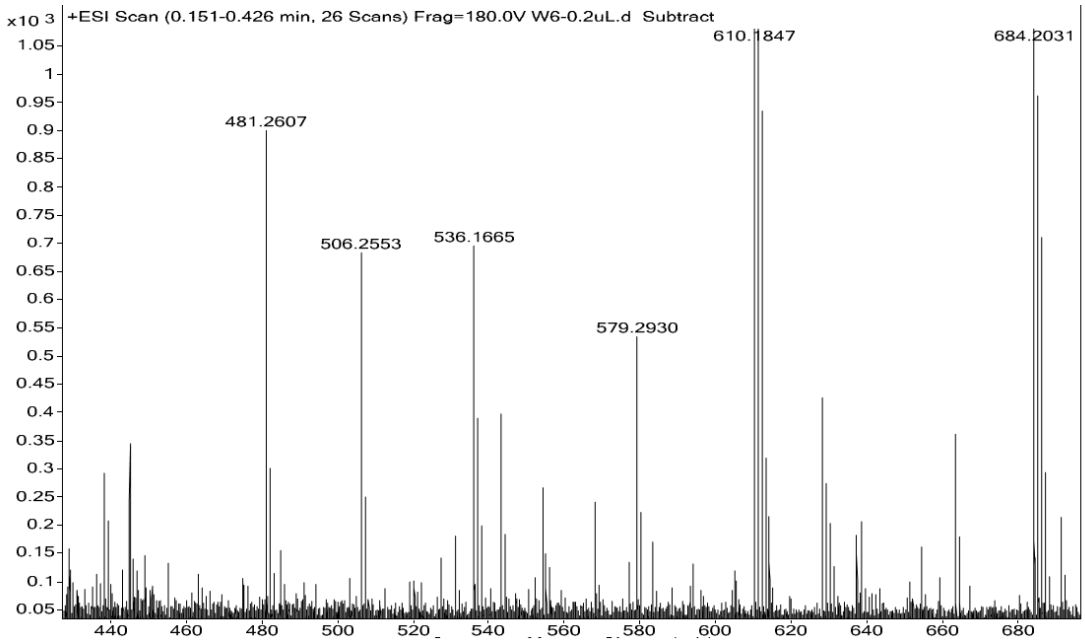

Fig. S19. HR-MS of $\mathbf{L_1}$ in the presence of Cr^{3+} in CH_3CN/H_2O (95:5, v/v) solution.

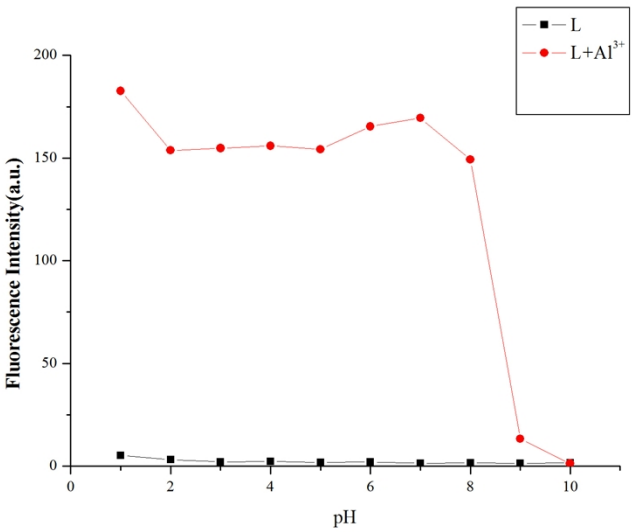

Fig.S20. Fluorescence intensity (582 nm) of free chemodosimeter $\mathbf{L}_1$ (10 μM) and in the presence of 10 equiv. Al^{3+} in CH_3CN/Tris-HCl (95:5, v/v) solutions with different pH conditions.

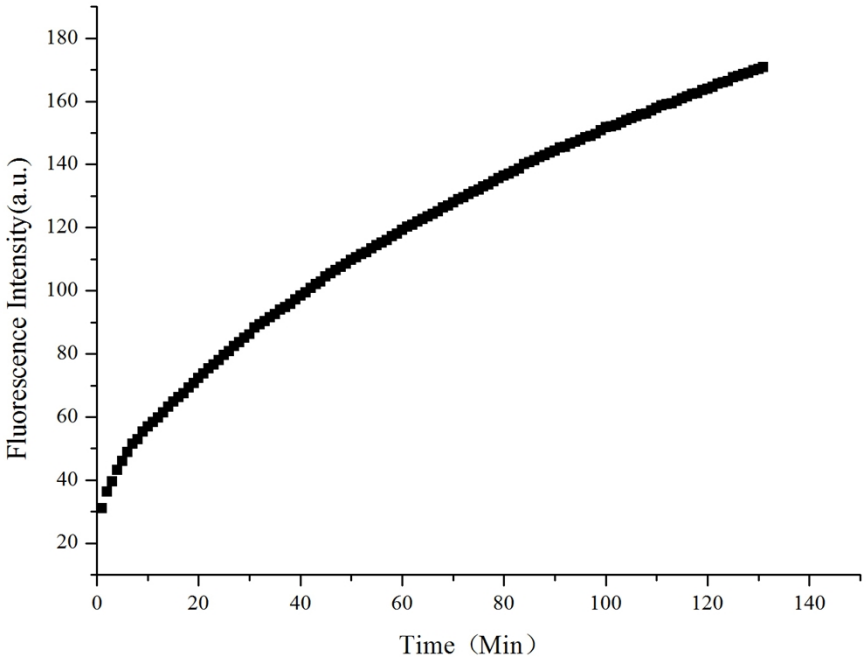

Fig.S21. Kinetics of the fluorescence enhancement of $\mathbf{L_1}$ (10 μM) in CH3CN/H2O (95:5, v/v) solution with the presence of 10 equiv. of Al^{3+}. Fluorescence intensity was recorded at 582 nm (λex = 520 nm, slit = 5 nm).

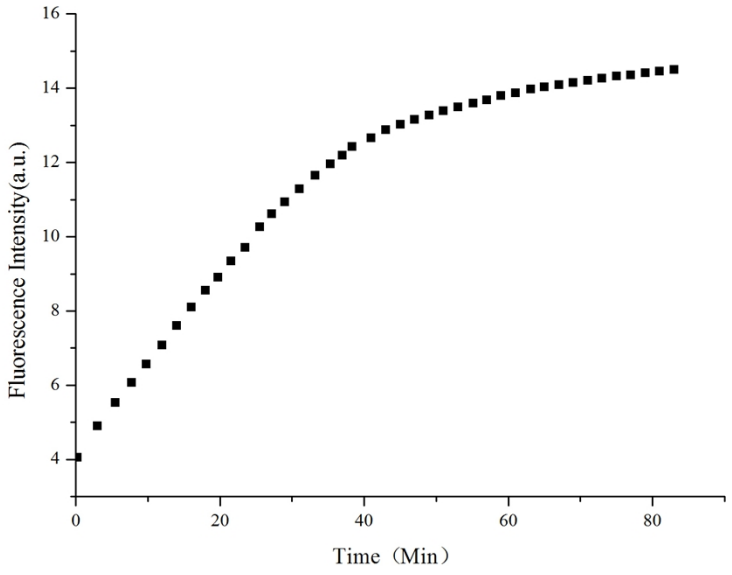

Fig.S22. Kinetics of the fluorescence enhancement of $\mathbf{L_1}$ (10 μM) in CH3CN/H2O (95:5, v/v) solution with the presence of 10 equiv. of Fe^{3+}. Fluorescence intensity was recorded at 582 nm (λex = 520 nm, slit = 5 nm).

Table S1. Determination of Al^{3+} Concentrations in Water Samples.

sample	Al3+ spiked (μM)	Al3+ recovered (μM)	Recovery (%)
Jinshui River water	0	not detected	
	25	4.87	19.48%
	50	13.6	27.20%
	100	24.81	24.81%

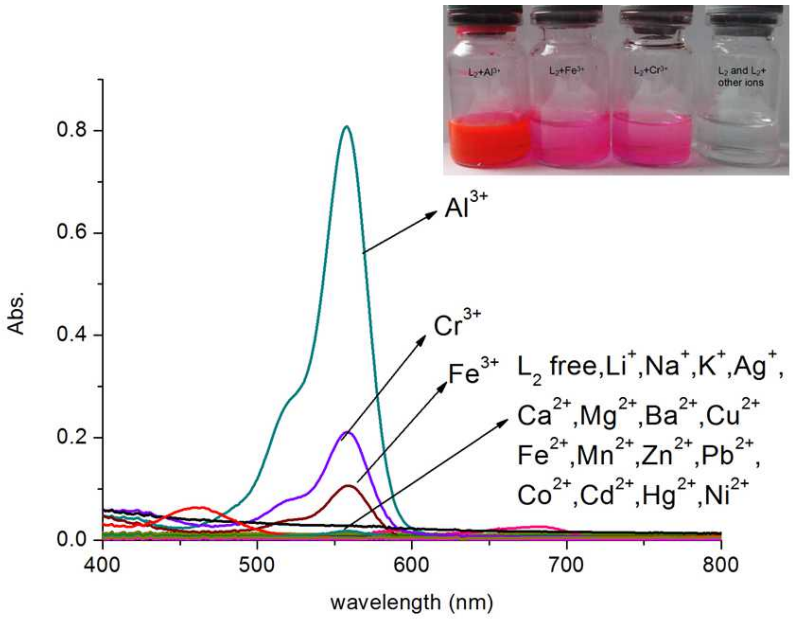

Fig. S23. Absorbance spectra of $\mathbf{L_2}$ (10 μM) in CH_3CN/H_2O (95:5, v/v) solution with the presence of 10 equiv. of various species. Inset: the photos of $\mathbf{L_2}$ with different metal ions in CH_3CN/H_2O (95:5, v/v) solution.

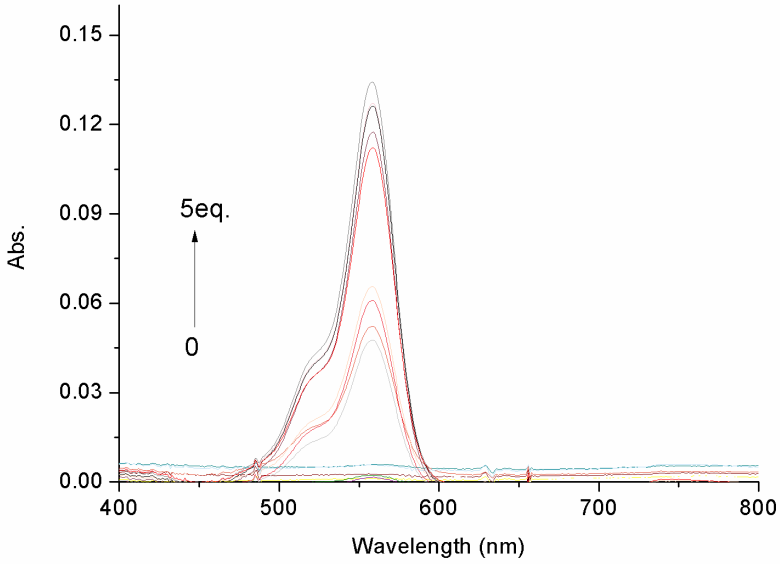

Fig. S24. Absorbance spectra of $\mathbf{L_2}$ (10 μM) in CH_3CN/H_2O (95:5, v/v) upon addition of different amounts of Al^{3+}.

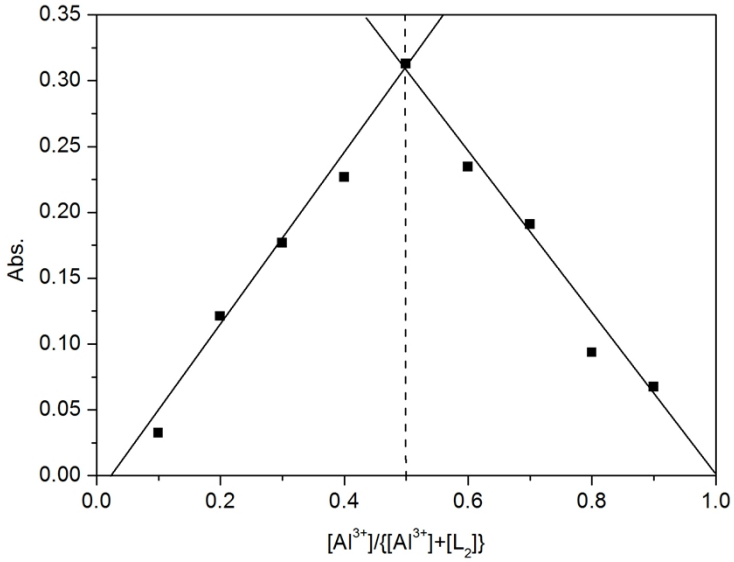

Fig. S25. Job's plots of the complexation between $\mathbf{L_2}$ and Al^{3+}. Total concentration of $\mathbf{L_2}$ + Al^{3+} was kept constant at 100 μM.

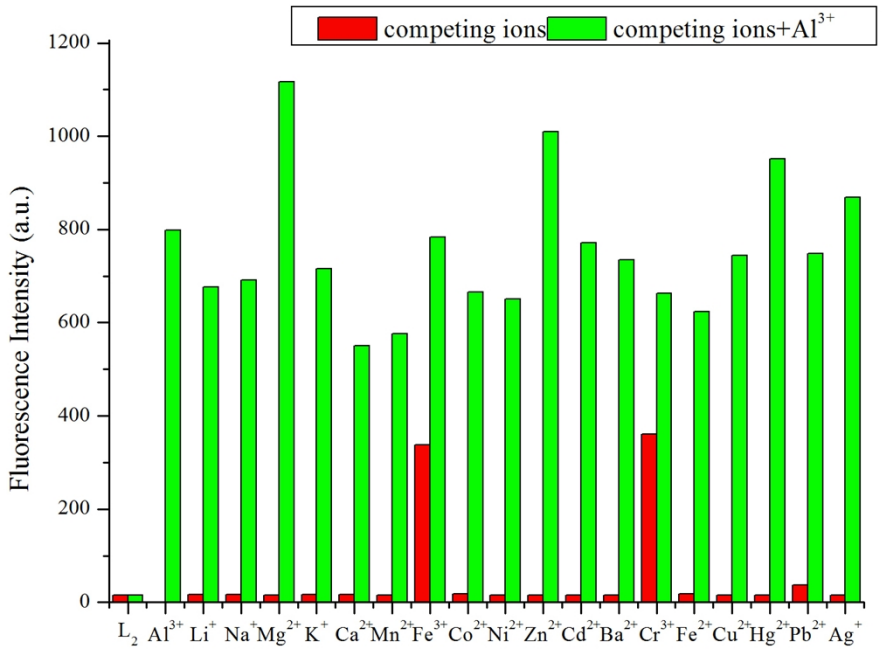

Fig. S26. Fluorescence intensity (at 582 nm) of $\mathbf{L_2}$ upon the addition of 100 μM Al^{3+} in the presence of 100 μM background metal ions in CH_3CN/H_2O (95/5, v/v), λex = 520 nm, slit = 5 nm

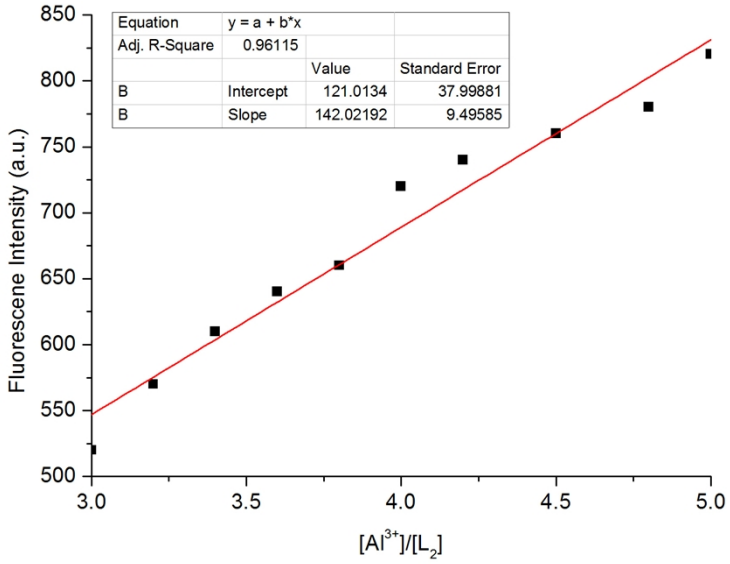

Fig. S27. The fluorescence intensity (at 582 nm) of compound $\mathbf{L_2}$ (10 μM) as a function of the Al^{3+} concentration (30-50 μM) in CH_3CN/H_2O (95/5, v/v) solution.

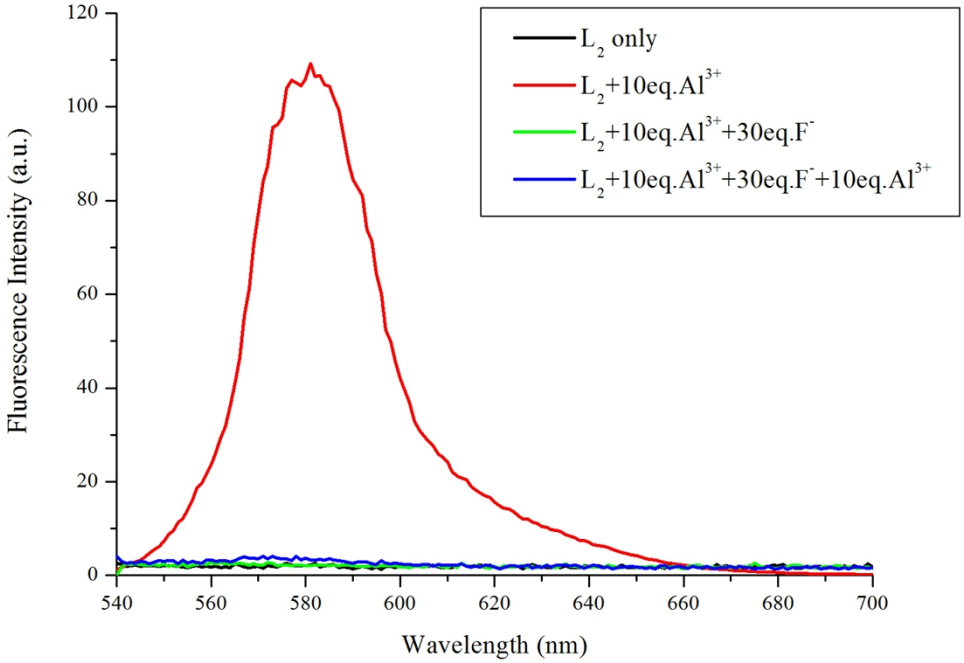

Fig. S28. Fluorescence intensity (at 582 nm) of $\mathbf{L_2}$ (10μM) to Al^{3+} in CH_3CN/H_2O (95:5,v/v) solutions (1) Baseline: 10 μM $\mathbf{L_2}$ only; (2) red line: 10 μM $\mathbf{L_2}$ with 10 equiv. Al^{3+}; (3) green line: 10 μM $\mathbf{L_2}$ with 10 equiv. Al^{3+} and then addition of 30 equiv. F^-; (4) blue line: 10 μM $\mathbf{L_2}$ with 10 equiv. Al^{3+} and 30 equiv. F^- then addition of 10 equiv.Al^{3+} (λex = 520 nm, slit = 5 nm).

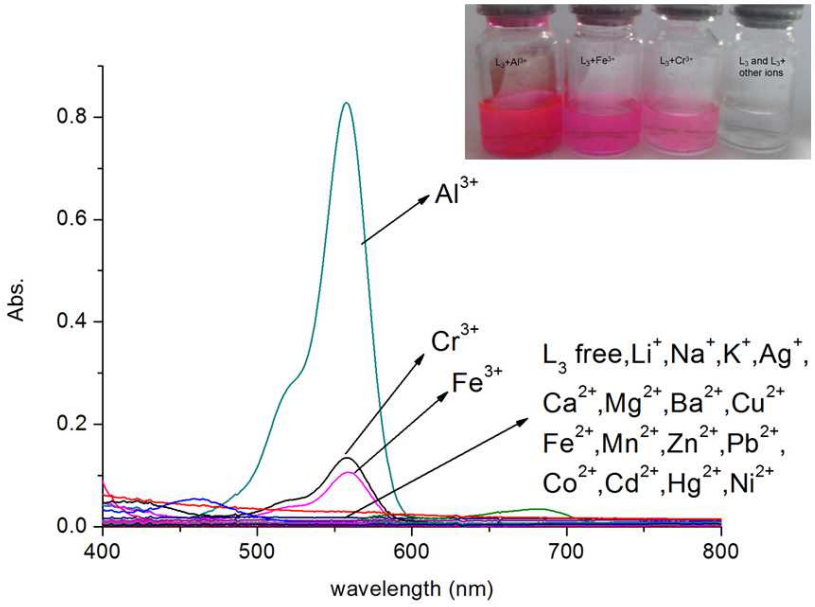

Fig. S29. Absorbance spectra of $\mathbf{L_3}$ (10 μM) in CH_3CN/H_2O (95:5, v/v) solution with the presence of 10 equiv. of various species. Inset: the photos of $\mathbf{L_3}$ with different metal ions in CH_3CN/H_2O (95:5, v/v) solution.

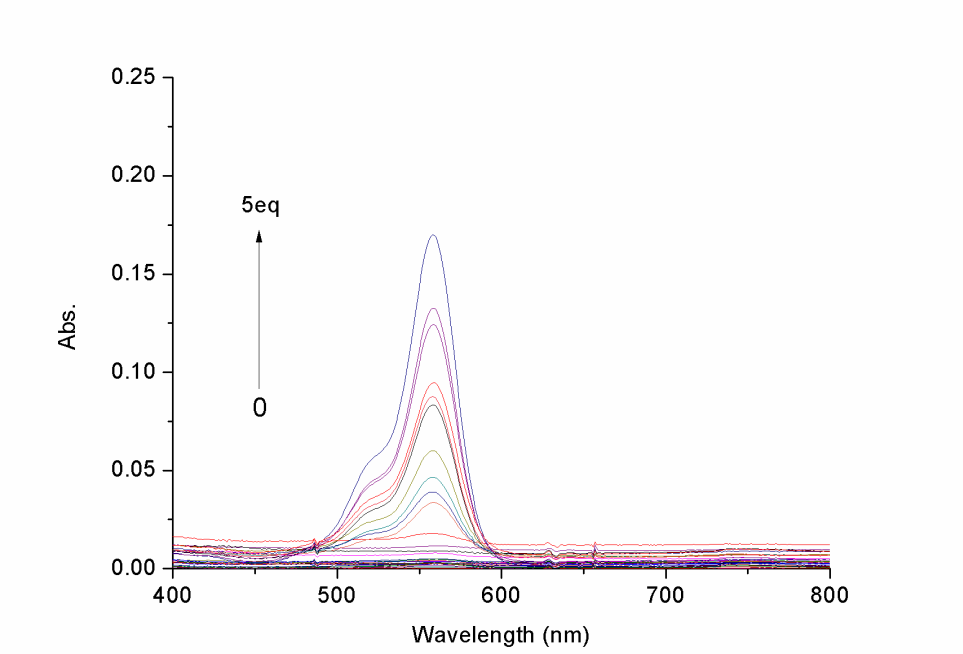

Fig. S30. Absorbance spectra of $\mathbf{L_3}$ (10 μM) in CH_3CN/H_2O (95:5, v/v) upon addition of different amounts of Al^{3+} ions.

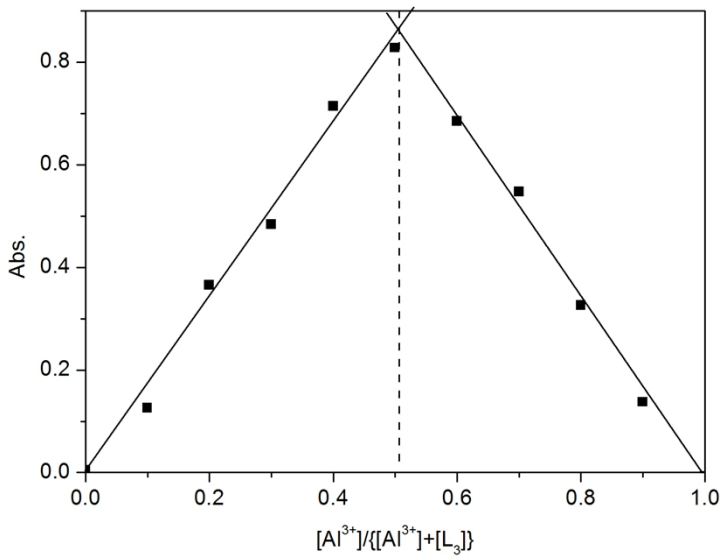

Fig. S31. Job's plots of the complexation between $\mathbf{L_3}$ and Al^{3+}. Total concentration of $\mathbf{L_3}$ +Al^{3+} was kept constant at 100 μM.

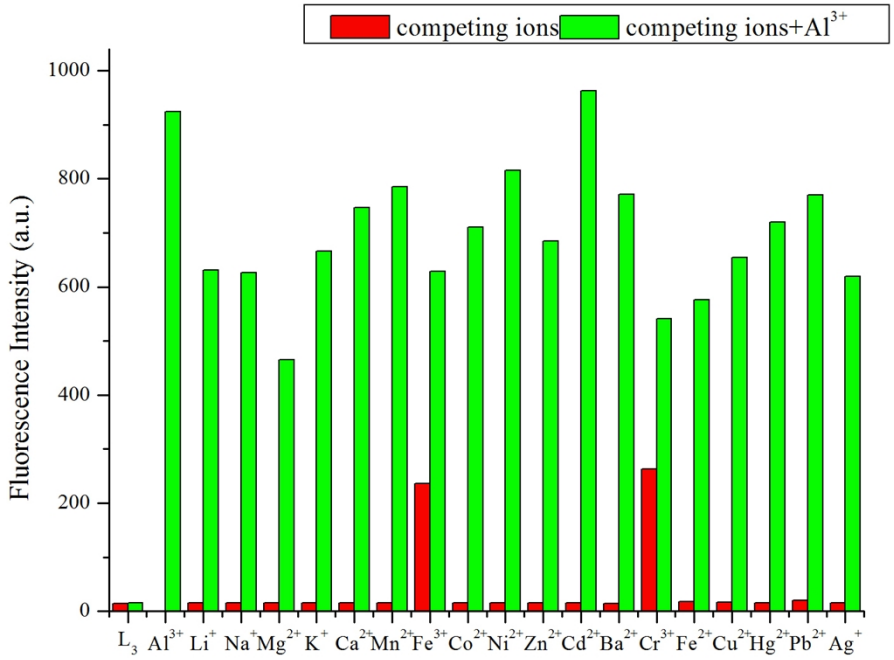

Fig. S32. Fluorescence intensity (at 582 nm) of $\mathbf{L_3}$ upon the addition of 100 μM Al^{3+} in the presence of 100 μM background metal ions in CH_3CN/H_2O (95/5, v/v), λex = 520 nm, slit = 5 nm.

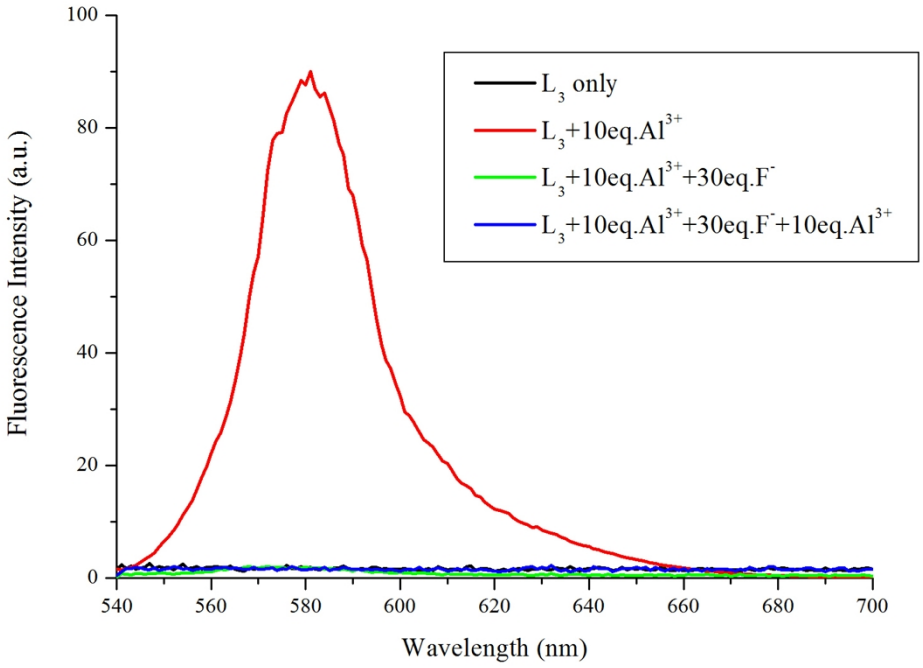

Fig. S33. Fluorescence intensity (at 582 nm) of $\mathbf{L_3}$ (10μM) to Al^{3+} in CH_3CN/H_2O (95:5,v/v) solutions (1) Baseline: 10 μM $\mathbf{L_3}$ only; (2) red line: 10 μM $\mathbf{L_3}$ with 10 equiv. Al^{3+}; (3) green line: 10 μM $\mathbf{L_3}$ with 10 equiv. Al^{3+} and then addition of 30 equiv. F^-; (4) blue line: 10 μM $\mathbf{L_3}$ with 10 equiv. Al^{3+} and 30 equiv. F^- then addition of 10 equiv. Al^{3+} (λex = 520 nm, slit = 5 nm).

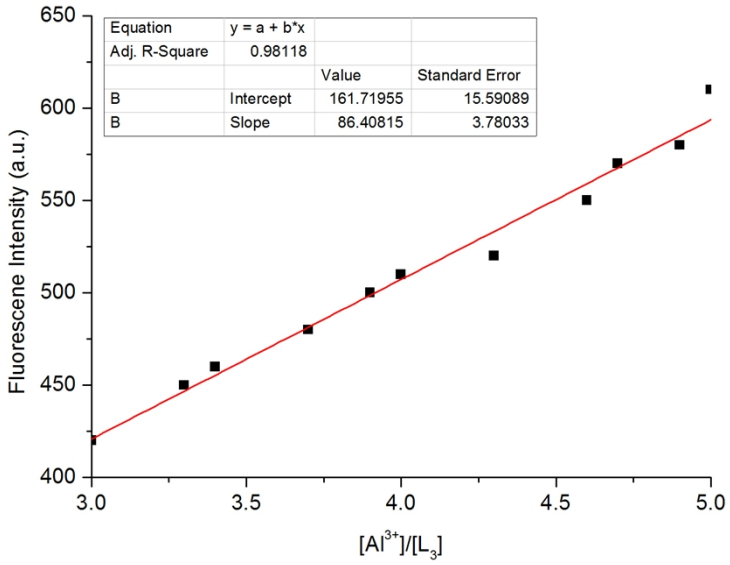

Fig. S34. The fluorescence intensity (at 582 nm) of compound $\mathbf{L_3}$ (10 μM) as a function of the Al^{3+} concentration (30-50 μM) in CH_3CN/H_2O (95/5, v/v) solution.